An Open Source GIS Tool to Quantify the Visual Impact of Wind Turbines and Photovoltaic Panels

Names of the authors.

Annalisa Minelli[a], Ivan Marchesini[b], Faith Taylor[c], Pierluigi De Rosa[d], Luca Casagrande[e], Michele Cenci[f]

[a] Insitute Universitaire Européen de la Mer - Université de la Bretagne Occidentale; Rue Dumont D'Urville, 29280 Plouzané, France.

email: Annalisa.Minelli@univ-brest.fr

[b] **(Corresponding Author)** National Research Council (CNR) - Research Insitute for geo-hydrological Protection (IRPI); Strada della Madonna Alta 126, 06125 Perugia, Italy.

email: Ivan.Marchesini@irpi.cnr.it

telephone:

[c] Earth and Environmental Dynamics Research Group, Department of Geography, King's College London, Strand, London, WC2R 2LS, United Kingdom.

email: Faith.Taylor@kcl.ac.uk

[d] Physics and Geology Department - University of Perugia; Via Zefferino Faina 4, 06123 Perugia, Italy.

email: Pierluigi.Derosa@unipg.it

[e] GFOSSERVICES S.A. - Open Source GIS-WebGIS solutions, Spatial Data Infrastructures, Planning and Counseling; Via F.lli Cairoli 24, 06127 Perugia, Italy.

email: Luca.Casagrande@gfosservices.it

[f] Servizio Energia qualità dell'ambiente, rifiuti, attività estrattive - Regione Umbia; Corso Vannucci 96, 06121 Perugia, Italy.
email: mcenci@regione.umbria.it

Author profiles

Eng. Annalisa Minelli is a post-doc researcher at the Institute Universitaire Européen de la Mer (IUEM), Technopôle Brest-Iroise, France.
Her research is mainly focused on GIS, geostatistical and trend analyses applications, recently applied to coastal zones and in the past applied to river dynamics. She is also skilled in geographical modeling using a variety of Open Source GIS software. One of her main interests is spreading the philosophy of Open Source.

Ivan Marchesini is a researcher at the Research Institute for Geo-Hydrological Protection (IRPI) of the National Research Council (CNR) of Italy.
He is a Geologist with a PhD in Geomorphology and Hydrogeology.
He also has a long background of geospatial analysis through Open Source GIS which he has exploited in different fields of applied research such as fluvial geomorphology, slope processes and mines reclamation.

Faith Taylor is a PhD student in the Earth and Environmental Dynamics Research Group within the Department of Geography, King’s College London. She is a physical geographer by training, focusing on modelling, GIS, remote sensing and statistical techniques applied to natural hazards. Her most recent research looks at building an Open Source, low data requirement model to forecast the impact of triggered landslide events on road networks.

Abstract:

Although there are clear economic and environmental incentives for producing energy from solar and wind power, there can be local opposition to their installation due to their impact upon the landscape. To date, no international guidelines exist to guide quantitative visual impact assessment of these facilities, making the planning process somewhat subjective. In this paper we demonstrate the development of a method and Open Source GIS tool to quantitatively assess the visual impact of these facilities using line-of-site techniques. The methods here build upon previous studies by (i) more accurately representing the shape of energy producing facilities (ii) taking into account the distortion of the perceived shape and size of facilities caused by the location of the observer (iii) calculating the possible obscuring of facilities caused by terrain morphology (iv) allowing the combination of various facilities to more accurately represent the landscape. The tool has been applied to real and synthetic case studies and compared to recently published results from other models, and demonstrates an improvement in accuracy of the calculated visual impact of facilities. The tool is named r.wind.sun and is freely available from GRASS GIS AddOns.

Keywords: visual impact, photovoltaic panels, wind turbines, landscape, GRASS GIS

1. Introduction

Over the 21st century, global demand for energy is expected to double, arguably requiring growth in renewable energy production such as solar (photovoltaic panel) and wind turbines to reasonably meet demands (Lewis and Nocera, 2006). Although there are clear benefits to these renewable technologies, uptake does not match potential of renewable energy production for a variety of reasons (Painuly, 2001). At a local scale, one such barrier is the aesthetic impact of renewable energy facilities on the landscape (Wüstenhagen et al., 2007). Hence, there is a clear need to carefully locate wind farms and photovoltaic panels to minimise their visual impact and increase social acceptance.

At present, there is not a unilaterally agreed, standardized method to quantify the visual impact of photovoltaic fields and wind farms. Landscape quality evaluations may rely upon local guidelines (Hurtado et al., 2003; Regione Autonoma della Sardegna, 2008), good practice manuals (Landscape Institute, Environmental Management Assessment, 2002; Scottish Natural Heritage et al., 2006; Vissering et al., 2011), survey-based or index methods (Ladenburg, 2009; Tsoutsos et al., 2009), and/or colour and light based methods (e.g., blending with the landscape) (Bishop and Miller, 2007; Chiabrando et al., 2011; Shang and Bishop, 2000).

Typically, the visual impact of a range of environmental phenomena is assessed through viewshed analysis in a GIS. In this method, a digital elevation model is used to determine which parts of the landscape are visible or not visible from a particular vantage point (Longley et al., 2010). For instance, studies have been carried out on the visibility of *Nuraghes* (De Montis and Caschilli, 2012)- native buildings from the Isle of Sardinia in Italy, on the visibility of electric transmission towers (Turnbull and Gourlay, 1987), on the maximisation of the scenic viewpoints along a touristic road (Chamberlain and Meitner, 2013). Manchado et al., (2013) recently reviewed computer programs available to perform visibility analysis for a variety of purposes.

Visibility analysis techniques have been applied to evaluate solar panel and wind turbine visibility (e.g. Moeller, 2006 and references therein). We build upon this work by taking into account the how the perceived size and shape of an object becomes distorted depending on the viewing point. An object's shape distortion as perceived by a human eye can affect the quantification of the area affected by visual impact on landscape perception, as we demonstrate.

This method is based on the concepts of (i) Visibility Analysis (Manchado et al., 2013) and Visual Magnitude (Chamberlain and Meitner, 2013), (ii) human eye perception and its field of view (Costella, 1992; Spector, 1990) and (iii) descriptive geometry (De Rubertis, 1979).

Quantitative analysis of visual impact is performed by (i) computing the field of view of an observer at a specific distance, (ii) evaluating the object

shape distortion perceived by a human eye, (iii) analysing the mutual relation between object, observer and earth morphology. The tool is developed as an add-on module for GRASS GIS, an Open Source GIS software (Neteler and Mitasova, 2008). As the code is completely available, users can freely read, verify, redistribute and modify the code, meaning that the tool is both flexible and that the reproducibility of results is guaranteed (Ince et al., 2012).

2. Material and methods

The tool developed is named "r.wind.sun". It is coded in the Python programming language (Van Rossum and Drake, 2001) as an add-on module to GRASS GIS, an Open Source GIS software (Neteler and Mitasova, 2008). The tool builds upon the existing GRASS GIS tool "r.viewshed" (Toma et al., 2010) which is based on the concept of Line of Sight (LOS); the straight line between the observer and object (e.g., Molina-Ruiz, 2011).

In the r.wind.sun tool, visual impact is quantified by the proportion of the field of view that is obstructed by the wind turbine or photovoltaic panel. This builds upon previous work by Rodrigues et al. (2010) that measures visual impact as the size of the observed object and half of the full solid angle multiplied by the square of the distance between the object and the observer.

In this section we introduce the key concepts applied to (i) calculate the field of view (ii) calculate the perceived size of objects within the field of

view (iii) calculate the ratio between the perceived size of object and the field of view and demonstrate that this is independent of distance. In section 2.3 we define the visual impact index and then show the development of the tool to measure this.

2.1. The human Field of View

In this section we define the shape and size of the region that can be seen by an observer, this is the human field of view (FOV). The "static" FOV is defined by three angles (Figure 1):

- nasal (n): measuring 85°, starting from the nose of the observer and extending outwards across a horizontal plane (Figure 1a).
- superior (s): vertical angle, measuring 65°, starting from the nose of the observer and extending upward (Figure 1b).
- inferior (i): vertical angle, measuring 70°, starting from the nose of the observer and extending downward (Figure 1b).

These angles define the region seen by at least one eye.

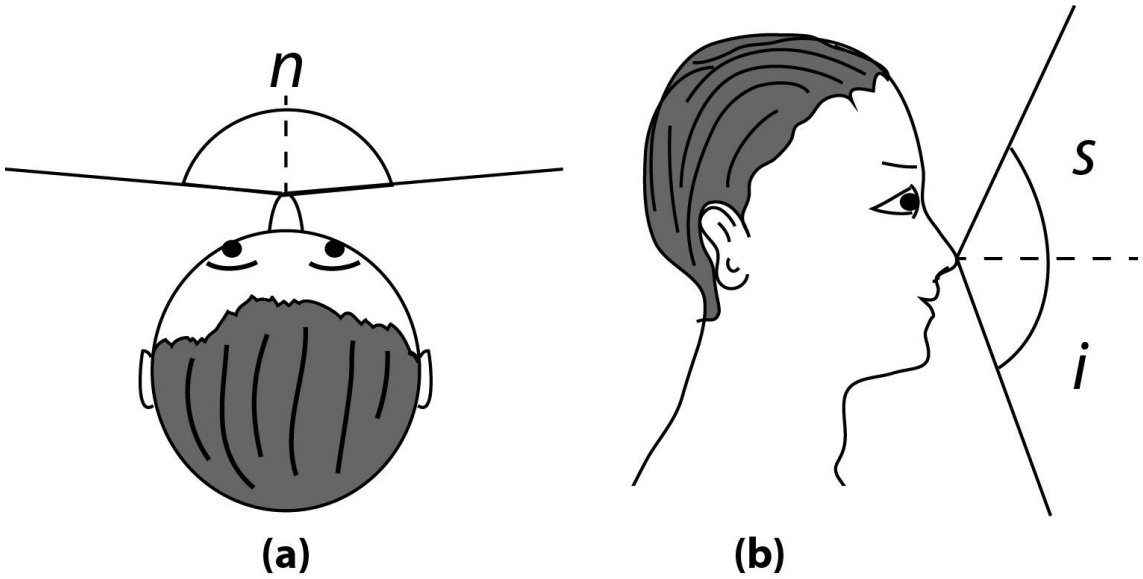

Figure 1. The angles that define the static human FOV. (A) n is the nasal angle defining a horizontal plane of 170° from the nose. (B) s and i are the superior and inferior angles defining lines extending 65° upwards and 70° downwards respectively from a horizontal line extending from the nose. When combined, these angles form an ellipse that defines the static FOV, shown in Figure 2.

The virtual field of view area (A_{fov}) depends on the distance (d) between the observer and object. The shape of the virtual field of view is an irregular ellipse of which the dimensions can be estimated by simple trigonometric relations.

Different values can be taken for angles s, i and n (e.g., considering only the full binocular part of the field of view, Spector - 1990). However, small changes to the values of these angles would cause only general scaling of the results without altering their meaning and the ratio between them.

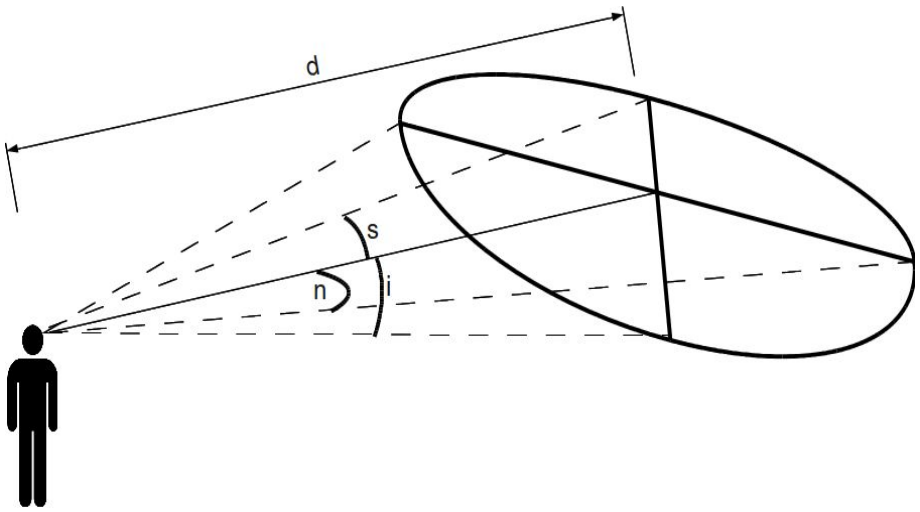

Figure 2: The static field of view.

If we now take into account the ability of the observer to move about a fixed point, we introduce two types of "dynamic field of view": "cylindrical" and "spherical".

In the first case, the observer can rotate their sight by 360° on the horizontal plane. Consequently, the elliptical shape of the field of view becomes the internal (lateral) area of a cylinder (Figure 3).

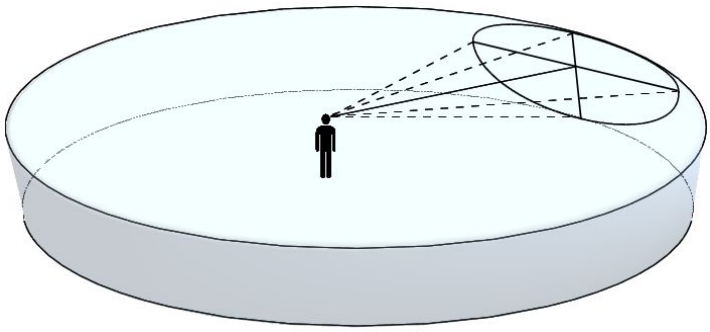

Figure 3: The dynamic cylindrical field of view.

In the second case, we extend this idea by assuming that the observer is able to move their sight in a vertical direction. The area of the field of view then becomes the internal area of a sphere (Figure 4).

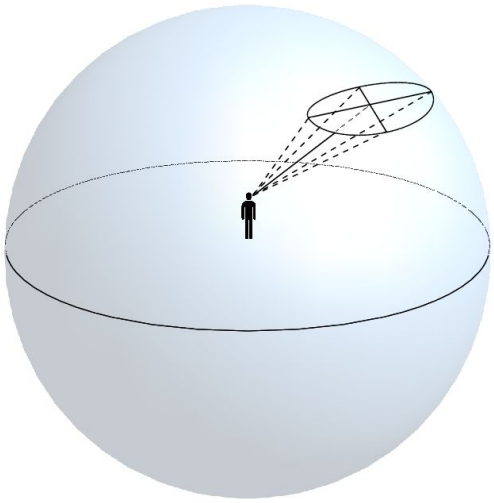

Figure 4: The dynamic spherical field of view.

As photovoltaic panels generally have a low/flat profile, the dynamic cylindrical FOV approach is used to calculate their visual impact. Whereas, the vertical dimension of wind turbines is not negligible and thus the dynamic spherical FOV approach is applied to calculate their visual impact.

2.2. The perceived shape and size of an object

The *perceived* size and shape of an object will differ to its *true* dimensions depending on the position (distance and angle) between the object and the observer. In Section 2.2.1 we demonstrate how the perceived size of an object is calculated. In Section 2.2.2, we demonstrate that when the

perceived size is represented as the proportion of the field of view occupied by an object, this becomes independent of the distance between the observer and the object. This allows us to combine multiple objects at different distances to calculate the overall visual obstruction (outlined in Section 2.2.3). Sections 2.2.1 - 2.2.3 principally discuss these calculations applied to a simple geometric shape. In Section 2.2.4 we explain how the true shape of wind turbines and photovoltaic panels can be simplified into a set of geometric shapes so these calculations can be applied.

2.2.1 Perceived Size of an Object

In Figure 5a we show how the dimensions of an object vary depending on the position of the observer. The observer is looking at a straight black pole with a "true" height (L) and "true" diameter (W). The observer is at an oblique angle (α) and distance (p) from the pole. In this example, the projective plane (A_{fov}) is centred on the pole at distance d (in this case, $d = p$). The perceived area of the object (l_a) is equal to the perceived length (l) × perceived width (w).

The degree to which the perceived area of the object is distorted from the "true" dimensions is dependant upon:

- the angle (α); the greater the angle between the observer and the pole, the smaller the perceived length (l) and consequently, the perceived area ($l \times w = l_a$). In particular when α=0, then l=L and when α=90, then $l = w$.

- the distance (p); the greater the distance between the observer and the centre of the pole, the smaller the object appears relative to the FOV (i.e., the ratio l_a/A_{fov}).

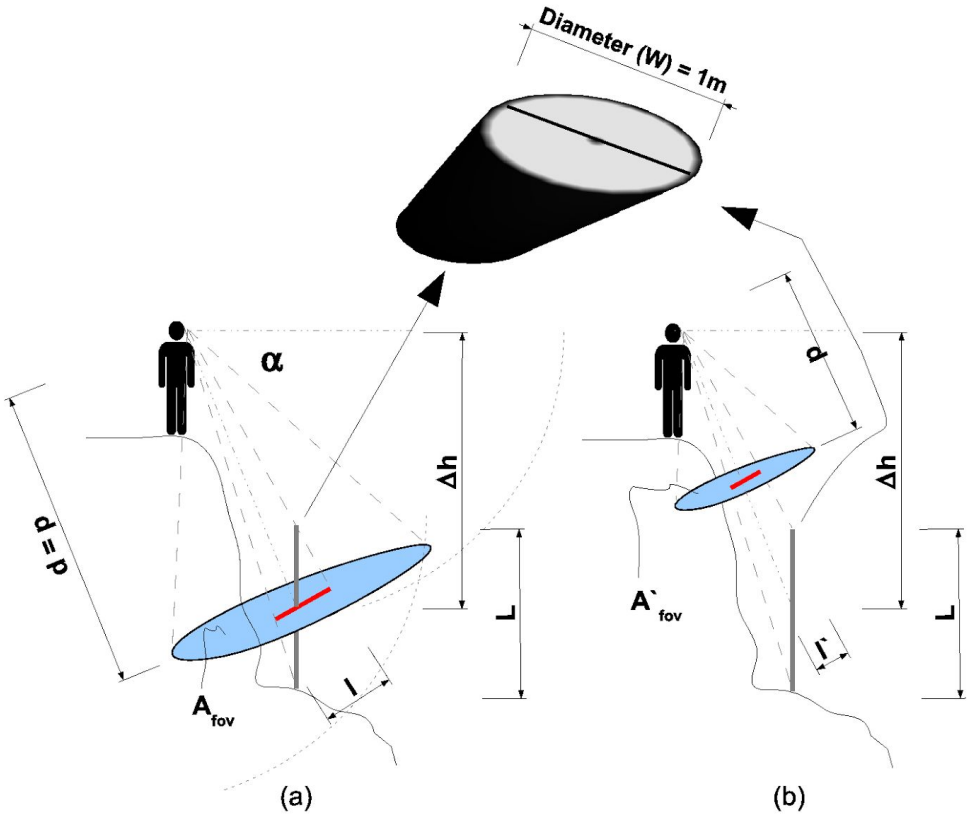

Figure 5: Change in perceived height (l) of an object with different placement of the projective plane (A_{fov}) (a) the projective plane is centered on the object at distance d. (b) the projective plane is at a shorter distance, d'. Projective plane is denoted in light blue and perceived height in red. In both cases, the true dimensions of the object ($L \times W$) are the same and the observer is at distance p, angle α from the object.

2.2.2 Perceived Size as a Proportion of Area of Field of View

We can represent the perceived size of an object (l_a) as a proportion of the area of the field of view (A_{fov}), making a dimensionless measure l_a/A_{fov}. This is shown in Figure 5b, where all variables are the same as Figure 5a apart from the distance between the observer and the projective plane (d') (i.e., the observer is focusing at a shorter distance). Although the perceived length of the pole (l') is now shorter, the area of the field of view (A'_{fov}) is now smaller, and thus the ratio between the perceived area (l'_a) and the area of the field of view remains the same. Hence at a distance $d' \neq d$ we obtain that:

$$l'_a / A'_{fov} = l / A_{fov} \qquad (1)$$

2.2.3 Combining Multiple Objects at Various Distances

By measuring the perceived size of an object (l_a) as a proportion of the area of the field of view (A_{fov}) we can place the dynamic field of view at an "arbitrary" distance (d). This allows calculation of the perceived size of multiple objects which differ in distance from the observer (p). Figure 6 demonstrates this concept using the spherical dynamic field to estimate the observed areas (l_{a1} and l_{a2}) of two different objects. We then calculate the overall dynamic field of view obstruction as a cumulative effect of the visual obstruction of individual objects. Hence, in general:

$$\sum_{i=1}^{n} l_{a_i} / A_{sfov} \qquad (2)$$

where n is the number of objects, l_a is the observed area and A_{sfov} is the spherical dynamic field of view at a fixed distance d (arbitrarily chosen).

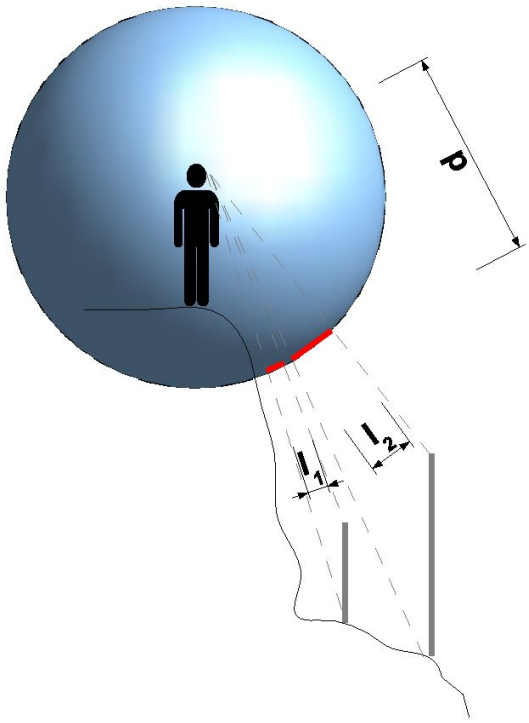

Figure 6: Estimating perceived size and overall field of view obstruction of two different objects placed at different distances from the observer. A dynamic spherical field of view is used in the example.

2.2.4 Calculating Perceived Size of Complex Shapes

The calculations in Sections 2.2.1 – 2.2.3 were applied to a simplistic example of a straight pole. Although the geometry of wind turbines and photovoltaic panels are more complex, most standard facilities can be simplified to sets of shapes and the same calculations applied.

A wind turbine can be split into two shapes: the tower can be represented as a trapezium and the rotor blades as a filled circle (which takes into account the rotation of the blades). For simplification, the rotor blades are assumed to always be facing towards the observer (resulting in some overestimation of size from certain angles). As an observer moves closer to the wind turbine, the perceived shape of the rotor approaches a flattened ellipse (in the vertical dimension) (Figure 7). These two shapes are then projected, depending on the α angle and the distance *d*. The projected areas are then summed.

Figure 7: The observed geometry of an aerogenerator. The tower is represented as a trapezium and the rotor as a filled circle. Photo license: http://commons.wikimedia.org/wiki/File:Aerogenerator_No_5,_Drumderg_-_geograph.org.uk_-_1424342.jpg

The observed shape of a photovoltaic panel is always a parallelogram or a trapezium. It is therefore easy to calculate its projected area (i.e., the obstruction of the field of view) by evaluating the two main projected dimensions (height and width) and then multiplying them (Figure 8) to obtain the perceived area of the panel.

Figure 8: The perceived shape of the photovoltaic panel. Photo license: http://commons.wikimedia.org/wiki/File:Panell_fotovolt%C3%A0ic.jpg

In previous studies, the shape of wind turbines and photovoltaic panels has been abstracted from simply the height and width of each element, which overestimates the proportion of field of view disturbed. Moreover, previous studies did not take into account the distortion of these shapes when viewing from different angles. We estimate that these inaccuracies in shape estimation causes an approximate doubling of the impact upon the field of view. By taking into account a more realistic shape and distortion, we believe this method of visual impact quantification is more precise.

2.3. Visual Impact Index

We quantitatively define the non-dimensional visual impact index (*NI*) as the ratio of the two areas:

$$NI = A_{obj} / A_{fov} \qquad (3)$$

where:

A_{fov} is the area of the chosen field of view (fixed, cylindrical or spherical);

A_{obj} is the perceived area of the elements (photovoltaic panel or wind turbine).

When the observer can see multiple objects from one position, each object has a different distance (*p*) from the observer. However, the NI-index is independent of the distance between the observer and the projective plane (*d*) (Section 2.2.2). Consequently, *d* can be set to the distance between the observer and the nearest object. Then the other objects must be projected (dimensionally scaled using simple proportions) onto the same projective surface (A_{fov}). The total NI-index can be then calculated as the sum of all the NI-indices obtained from the different objects.

This index represents the percentage of impact (visual obstruction) produced by each single object in the field of view. In probabilistic terms, it represents the probability of visual impact from each single observation point: the ratio between positive events (when visual impact occurs) and all possible events.

2.4. Calculation

r.wind.sun is a Python script for GRASS GIS which evaluates the visual impact index (NI-index) for each cell of a raster map in the area surrounding one or more wind turbines or photovoltaic panels.

Required inputs are:

- a Digital Elevation Model (DEM);
- a vector point map giving the location of centroids of the wind turbines or photovoltaic panels;
- dimensions and inclination of the facilities;
- distance threshold parameters to define the zone of analysis.

2.4.1 Implementation for Wind Turbines

For each facility, the perceived area is calculated for all cells in a given radius around that facility. The radius is defined by the user as a "maximum distance" parameter. For each pixel within the radius, the dynamic spherical field of view (A_{fov}) is calculated where d is set to the minimum distance between that cell and the nearest wind turbine.

The r.wind.sun tool is able to take into account the impact of terrain morphology obscuring parts of each wind turbine. The tool schematically considers whether (i) only the upper half of the rotor is visible, (ii) the entire rotor is visible, (iii) the entire plant is visible. If the entire plant is visible, the tool estimates the sum of the perceived area of the rotor and of the tower to evaluate the perceived area of the wind turbine. If the tower or part of the rotor is obscured by the terrain, the perceived area is calculated as half of the perceived area of the rotor.

2.4.2 Implementation for Photovoltaic Panels

For the photovoltaic panels, the tool calculates the perceived area for all cells that lie within a "donut" shape centered about the facility, defined by minimum and maximum distance threshold parameters. The minimum distance parameter is used to avoid analysis being performed upon the facility itself, or in neighbouring cells also containing photovoltaic panels (as they tend to be grouped together). To calculate the perceived area of each facility, the tool uses a cylindrical dynamic field of view where *d* is equal to the distance from the nearest panel centroid.

2.4.3 Processing

From an algorithmic point of view, the analysis is performed sequentially upon each individual element (e.g., each single wind turbine). For each element, an individual raster map of the NI-index is generated. These maps are then summed together to obtain a final NI-index map for all facilities.

As the model is raster based, the processing time is strongly linked to the cell size and the maximum distance chosen to evaluate the visual impact (i.e., the size of the study region). Large values of the maximum distance and high spatial resolution strongly increase the processing time.

This has been an issue for raster analysis since the 1990s (Kinder et al., 1997). However, advances in software and technologies such as the optimization of algorithms has helped significantly in reducing the duration

of the analyses. For example, on a using a computer with 4Gb of RAM and a 2.0GHz processor running a Linux Operating System, applying the code to a study region with a maximum distance of 10 km from the facilities and a resolution of 10 m (more than 3 million cells) the analysis is completed in approximately 10 minutes. Moreover, the code could be parallelized in a way that GRASS GIS can process each wind turbine or panel in a different mapset.

2.4.4 Output

The main output of the r.wind.sun tool is a raster layer where the cells values represent the non-dimensional visual impact index (*NI*) value. There are various options for more detailed output from the tool. For example, if the user requires a three-dimensional view of the wind turbine, they can input a template (in .dxf format) of the facilities.

The values obtained for the impact index are often very small. Using the example of Figure 5a and 5b, it is clear that an increase of *d* (the distance from the projective plane), whilst maintaining a constant angle α does not result in large variations in I_a. However, it results in a substantial increase in A_{fov}. In our opinion, this is correct as it reflects the intuitive experience that an object apparently and rapidly "becomes small" when we moving away from it.

Detailed practical steps for installing and executing the tool are outlined in Appendices 1 - 3.

3. Case studies

We have tested the model using both synthetic (Section 3.1) and real data (Section 3.2). The first application with synthetic data aims to explore the distortion effect in the quantification of visibility. The second experiment then demonstrates the tool function in a real setting.

3.1. Synthetic case study

In this section we show a synthetic example of how r.wind.sun is able to take into account the effect of the perceived size of objects on the visual impact index. To accomplish this task we will show how this effect can influence the estimation of the maximum distance at which an object is visible and, as a consequence the landscape area affected by the visual impact.

Molina-Ruiz et al. (2011) define a method to quantify the maximum visible distance for a tall linear object (suitable for analysis of wind turbines but not photovoltaic panels). Rodrigues et al. (2010) report a development of this method which allows calculation of maximum visible distance using a simplified (rectangular) area of the observed object.

The literature review did not reveal any papers that considered the effect of distortion of the shape and size of the observed object on the estimation of its visual impact. So it is useful to use r.wind.sun to show how the visual impact of an wind turbine can be affected by the possibly altered shape perceived by an observer.

We can define the minimum resolvable size of an object at various distances by a 25 arc minute^2 solid angle (Shang and Bishop, 2000).

Rodrigues et al. (2010) state that the maximum distance at which the object remains visible can be expressed as is:

$$\Delta = \sqrt{\frac{I^w * I^h * c}{25}} = \sqrt{\frac{A_{obj} * c}{25}} \qquad (5)$$

where:

Δ is the maximum visible distance in meters;

$I^{w,h}$ are the "true" width and height of the observed object in meters;

A_{obj} is the "true" area of the observed object in square meters;

c is a constant which converts steradians to square minutes:

$$c = (180 * 60 / \pi)^2 \simeq 1.18 * 10^7 \qquad (6)$$

At distance Δ, for a well defined wind turbine or photovoltaic panel, it is possible to estimate the theoretical value of the NI-index, that we define as $TNI_\Delta = Aobj / Afov_\Delta$, where $A_{fov\Delta}$ is the area of the spherical or cylindrical field of view. This value can then be compared with that calculated using r.wind.sun (NI_Δ). In this case we compare the NI-values starting from distances, because as this is the most influencing variable on the NI-index calculation, the distance affects directly the final index value. However, comparing the two index values (the theoretical and that produced through r.wind.sun calculation at the same distance Δ) we can demonstrate that the r.wind.sun tool is able to take into account the effect of the perceived shape on the visual impact estimation.

The procedure to achieve this comparison is described in the flowchart in Figure 9 and it is principally composed of the following steps:

1. knowing the area (size) of the observed object, the maximum distance value (Δ) can be calculated using the equation (5).
2. using Δ as the r.wind.sun "maximum distance", it is possible to run r.wind.sun and calculate the NI-index map.
3. the values of the NI-index map at distance Δ, NI_{Δ}, can be compared with the theoretical values (TNI_{Δ}).

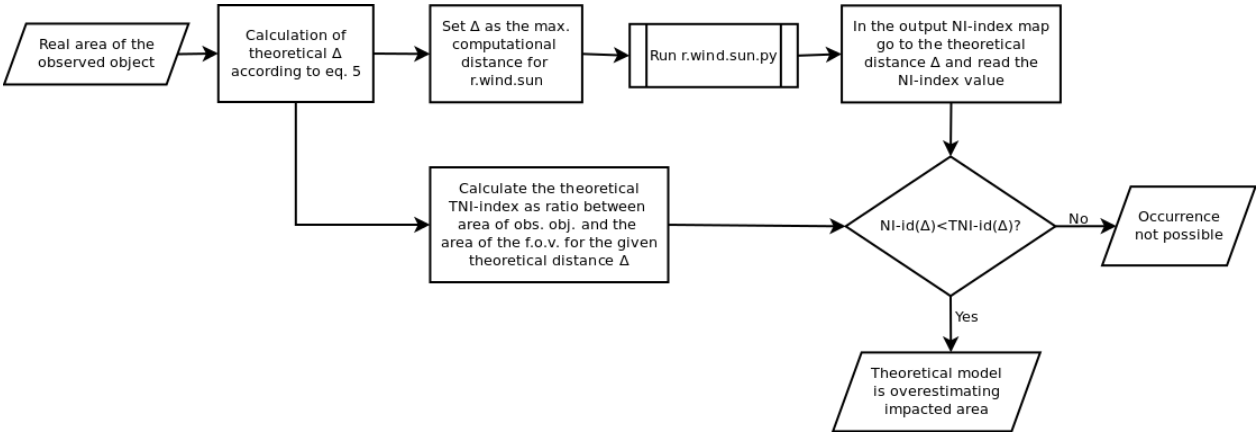

Figure 9: Flowchart of the comparison procedure.

To avoid any effects of partial obscuration of objects due to topography, two very simplistic synthetic topographies were created: one perfectly planar and the other very schematically mountainous. We acknowledge that the example is extreme and very artificial but it is used to demonstrate the capability of the model to calculate the effects of distortion of objects, and therefore should be considered only as a technical exemplification.

Applying this approach to a planar area and thus observing the object frontally (meaning, not considering the effect of optical distortion on the

object perception) the tool r.wind.sun verifies equation (5). The NI-index value obtained by the tool at Δ distance (NI_{Δ}), is almost the same as that calculated theoretically (TNI_{Δ}). In Figure 10, we show an example of the results obtained modeling a 100 m high wind turbine on planar topography. The total area of the aerogenerator (considering the rotor) is 10380.9 m^2. Following the previous steps:

1. the Δ distance is 6999.8 m ~ 7 km.
2. the NI-index map obtained through r.wind.sun is shown in Figure 12a.
3. The theoretical NI-index value (TNI_{Δ}) at the Δ distance is 1.68×10^{-5}, which means that the 0.00168% of the observer's spherical field of view is occupied by the wind turbine. Reading the map obtained using r.wind.sun, it can be verified that the impact value NI_{Δ} obtained at the Δ distance is equal to the TNI_{Δ} value (see Figure 12b).

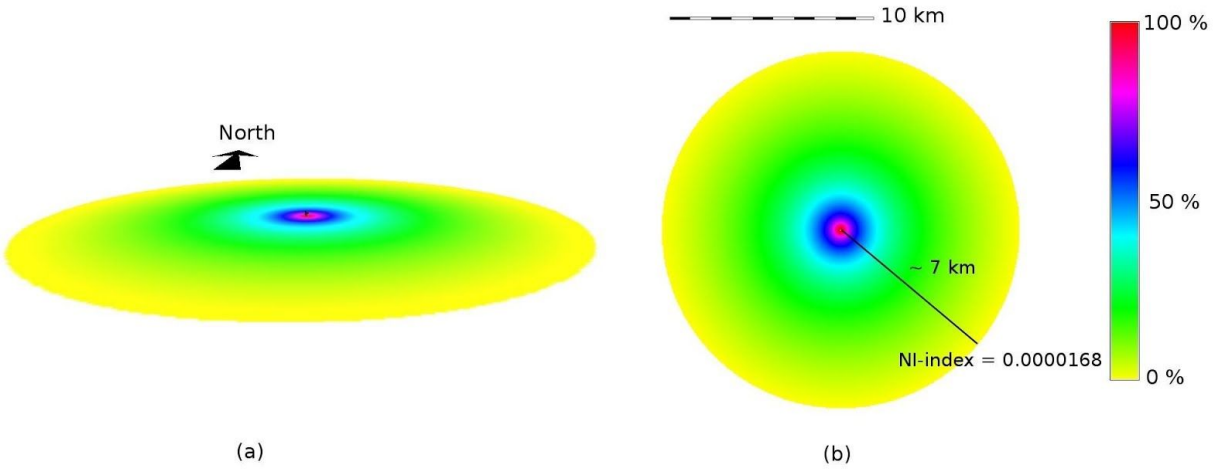

Figure 10. NI-index map obtained using r.wind.sun to model the aerogenerator visibility on a flat terrain. (a) 3D and (b) 2D views of the results.

Next, we introduce a regular slope (30° - Fig. 11a) in the topography. We decided to consider a very synthetic topography to demonstrate that perspective effects the evaluation of the visual impact whilst removing any confounding factors caused by topography.

In this case, we expect that the r.wind.sun NI-index equals the theoretical TNI_{Δ} at a distance $\Delta_m << \Delta_h$ where $\Delta_h = \Delta * cos(30)$.

In Figure 11 we show an example of the results obtained by modeling a 100 m high wind turbine and assuming a topography with a constant downward slope of 30° starting from the wind turbine. Following the previous steps:

1. the Δ distance remains 7 km but since it is inclined by 30°, corresponds to 6.06 km (Δ_h) in terms of horizontal distance.
2. a new NI-index map is generated using r.wind.sun and showed in Figure 11a.
3. The theoretical NI-index value (TNI_{Δ}) at the distance Δ_h remains the same as before (since the inclined 3D distance is 7 km as for the planar topography). However, in the map obtained using r.wind.sun, the NI-index value at the Δ_h distance is substantially lower: $NI_{\Delta} \sim 1.38 \times 10^{-5}$.

Moreover, analysing the NI-index map produced by the r.wind.sun module, it is possible to verify that the theoretical TNI_{Δ} value is achieved at a horizontal distance $\Delta_m \sim$ 5600 meters (Figure 11b). Δ_m was obtained by filtering the NI-index map in order to remove all the values less than $TNI_{\Delta h}$

and then measuring the maximum distance between the wind turbine and the remaining cells in the filtered NI-index map.

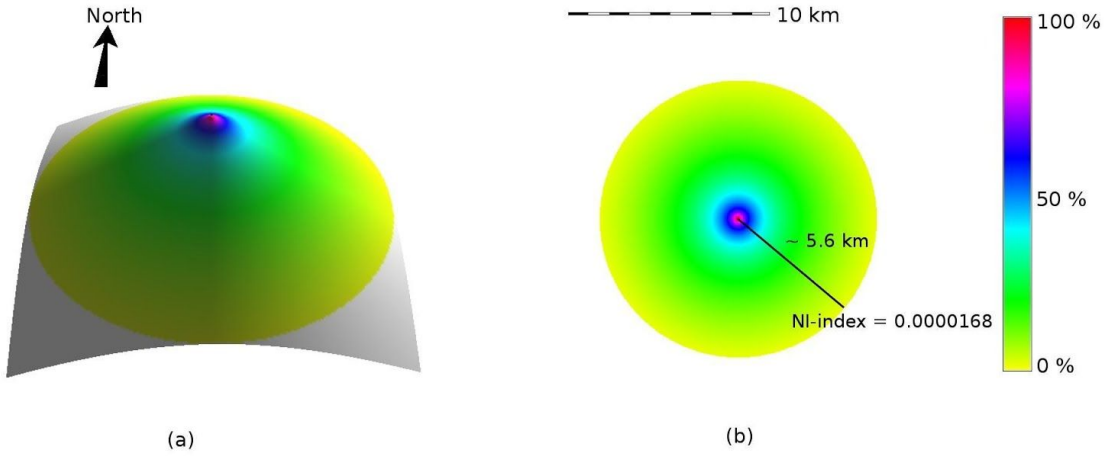

Figure 11. NI-index map obtained using r.wind.sun to model the wind turbine visibility on a constant-slope terrain. (a) 3D and (b) 2D views of the results. The colour scale is logarithmic.

The described results demonstrate that the r.wind.sun tool is able to take into account the effect of the perceived size on the visual impact.

Using simple GRASS GIS tools, it is possible to evaluate the circular area (circular crown) between the theoretical and practical distance considered (5.6 km and 6.06 km). This area represents an exact measure of "how much" the effect of the altered perceived size affects the estimation of the visual impact. In the above example this area is estimated to be ~16.9 km^2, i.e., 14.7% of the area that should be considered visually offended not considering the effective of perspective.

We believe that these considerations are useful for the practical applications of the tool such as landscape planning.

3.2. Real World Application: Cima Mutali

The tool was applied to two existing wind turbines, sited in "Cima Mutali", Fossato di Vico, Perugia, Italy. The NI-impact output map is shown in Figure 12a.

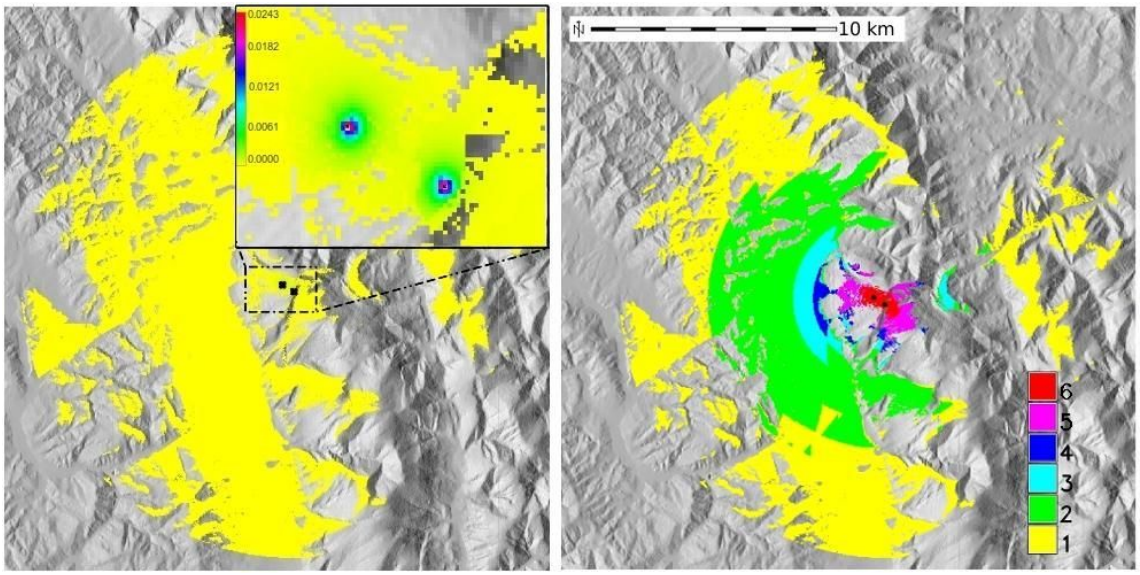

Figure 12: Visual impact map for wind turbines in Cima Mutali, Central Italy. a) the NI-impact index value and b) reclassification of the NI-impact into intensity bands: each band covers the same interval length of values.

Figure 12b shows the NI-index map reclassified into 6 equal interval bands values are divided into equal size intervals. A value of 1 denotes low impact and 6 maximum impact. The 3D image (Figure 13) of the reclassified impact map demonstrates how the tool is able to take into account the effect of the morphology in the partial obscuring of wind turbines.

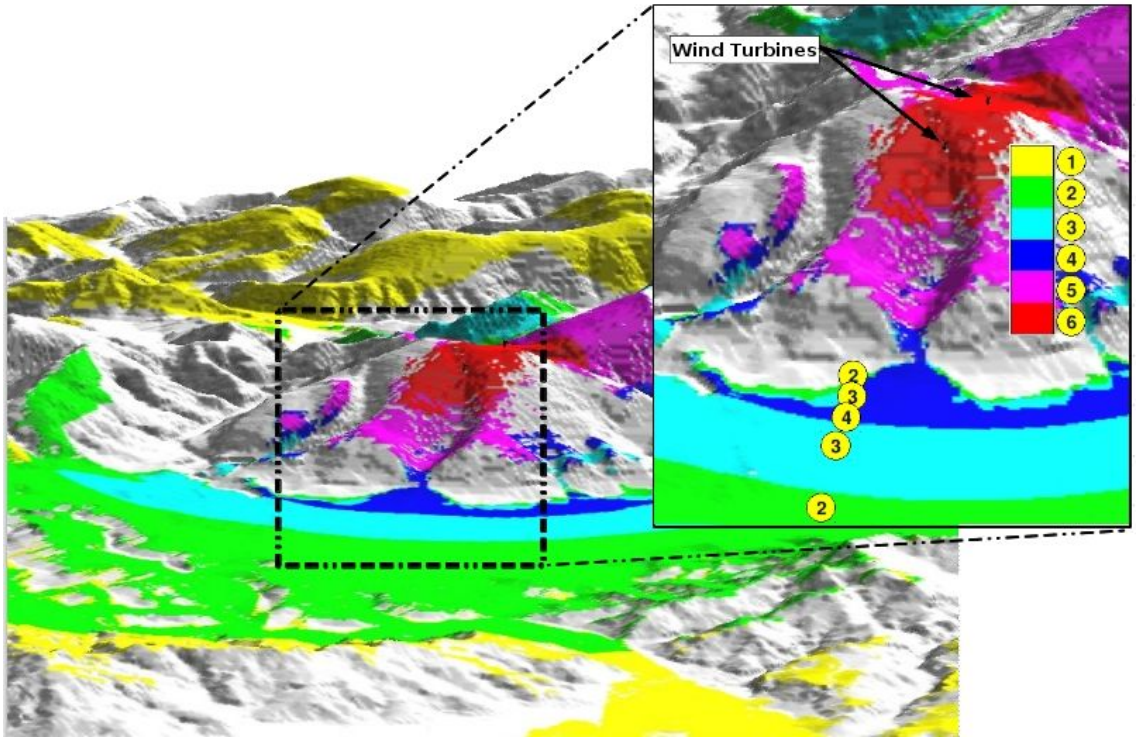

Figure 13: Three-dimensional view of the territory of Fig. 12: the landscape and a detail. The 3D is produced using the GRASS GIS tool NVIZ.

In the zoom box in Figure 13 we show that the NI-impact values increase from 1 to 6 (from yellow to red) as we move closer to the wind turbines. Areas with no colour denote zones where the wind turbines are not visible. There is a slight anomaly at the foot of the hill where visual impact actually decreases from 2 to 4 as we move towards the wind turbines. This is attributable to the fact that the hill only partially obstructs the wind turbines.

3.3 Intuitive Measures of Visual Impact for Decision Makers

The absolute values of the NI-index are not immediately understandable or intuitive. In this section, we describe a method to create a comparative scale which could be used to communicate the results of the model to decision makers and landscape planners.

To do this, we take a small object of known dimensions (in this example, an ISO A4 sheet of paper) and calculate at what distance (d_{A4}) the piece of paper would have to be placed from the observer to create the same visual obstruction as the wind turbine. This can be done by re-calculating the value of each single pixel of the output layer:

$$d_{A4} = \sqrt{\frac{A_{A4}}{4\pi * NI}} \qquad (4)$$

where NI=impact index, A_{A4}=area of an A4 paper.

We believe this method creates a more intuitive interpretation of the results and could be very useful for presenting to decision makers. In GRASS GIS this can be easily be performed using map algebra.

4. Discussion and conclusions

To date, there is no precise set of rules to quantitatively (geometrically) estimate the visual impact of wind and photovoltaic farms. Perhaps because of this, often more prominence is given to other factors such as social or agricultural impacts (Cerroni & Venzi - 2009, Rogge et al. - 2008). The tool we have developed here offers a more objective method to quantify this

impact numerically, allowing direct comparison between sites and scenarios, providing a useful tool for landscape planners.

Similar tools exist to quantify the visual impact based on line-of-sight principles (e.g., Molina-Ruiz et al., 2011; Rodrigues et al. 2010). However, due to the r.wind.sun model taking into account the effects of (i) the real 3D distance between the observer and the object and (ii) the distortion of size and shape caused by the human eye in concurrence with the presence of a non-planar terrain morphology, the output of the r.wind.sun model can be considered more accurate calculations of visual impact.

These simpler formulations based only on the planar distance between the observer the object work well in case of plain topographies but overestimate the visibility area in case of different terrain morphologies. When applied to real cases (when the morphology is not typically planar and the possibility that the observer could view the plant from oblique angles), the maximum visible distance is overestimated by these simpler formulas. This is due to the effect of the morphology (which can hide or partially obscure facilities), and to the effect of distortion of the perceived area by the observer's eye.

Nonetheless, the perceived dimension of an object is only a part of the visual impact that an object can cause. For instance, colouring can play an important role in determining the visibility of an object (Bishop and Miller, 2007). In this sense the tool r.wind.sun can be considered a preliminary answer to the question of providing a quantitative estimate of the visual impact of wind turbines and photovoltaic panels.

The adimensional nature of the tool developed here allows combination of results to more realistically simulate the visual impact of various facilities across a landscape (for instance, a combination of photovoltaic panels and wind turbines, or a large wind farm). Theoretically, this same approach could be used to estimate the visual impact of other major works/infrastructure in the same region (such as buildings, roads, quarries, forests etc.), assuming that it is possible to approximate their shape with simple geometrical models. This could bring a more integrated approach to the estimation of visual impact of man-made structures on a landscape.

Appendix 1

Tool availability

The tool r.wind.sun is available under the terms of the GNU GPL license as part of the GRASS GIS AddOns. The entire code and related documentation is available at:

https://svn.osgeo.org/grass/grass-addons/grass6/raster/r.wind.sun/.

An example model of a wind turbine to perform the intervisibility analysis of a windfarm can be found here:

http://www.gfosservices.it/wp/wp-content/uploads/2012/12/inputfile.txt.

To install the tool on GNU/Linux it is necessary to have GRASS GIS (version 6.4) compiled by source code or installed by package. The tool can be added using the g.extension tool. r.wind.sun depends on the r.viewshed tool that is also available through g.extension (Neteler, 2012).

A QGiS version of the software (working under the GRASS GIS plugin and on Windows) is in development (Quantum GIS Developement Team, 2012). More information on the availability of the tool on QGiS can be obtained by contacting the authors.

Appendix 2

Using the tool to calculate the NI-Index of Wind Turbines

The r.wind.sun tool can be executed directly from the GRASS GIS command line interface (CLI) or using the graphic user interface (Figure I).

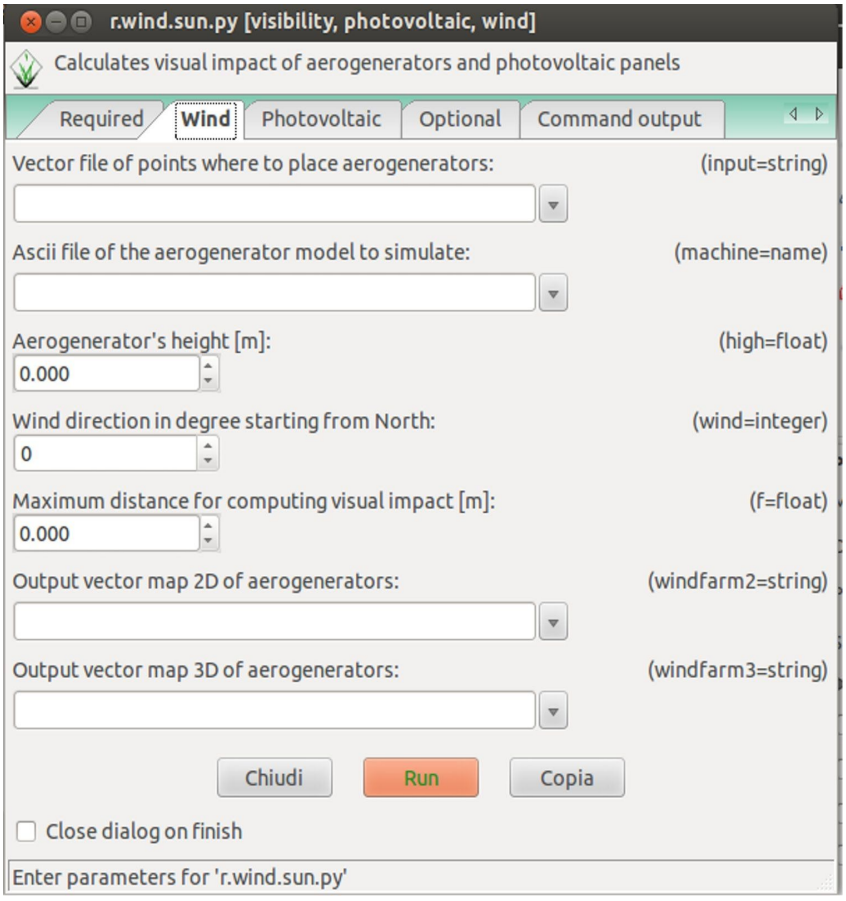

Figure I: The graphic user interface - "wind" tab.

When analysing a wind turbine's visual impact, one must select its related flag ("-w" using the CLI). Subsequently a digital elevation model (DEM) and the name of the output impact layer must be provided.

Other inputs required are:

- A point vector layer containing the position of the wind turbines;
- A three-dimensional model of the wind turbine, which can be different for each plant.
- The total height of the wind turbine (tower plus rotor);
- The prevalent wind direction, which must be measured starting from North and then proceeding clockwise;
- Maximum distance for computing the visual impact index.

Other outputs of the tool are:

- two-dimensional vector map of the wind turbines;
- three-dimensional vector map of the wind turbines.

These can be useful to produce cartography or the three-dimensional rendering of the analysis results. The wind direction does not affect the analysis and is only used for descriptive purpose. The 2D and 3D outputs (vector layers), show the wind turbine rotor oriented in that direction. The 3D vector map can be exported from GRASS GIS in different formats and imported in many of the available 3D rendering softwares (as an example to KML format to visualize the object in GoogleEarth).

Here we show an example of the string required to execute the tool from the CLI:

r.wind.sun -w dem=dem impact=impactMap input=placingPoints machine=inputfile.txt high=120 wind=45 f=10000 windfarm2=vect2d windfarm3=vect3d

Appendix 3

Using the tool to calculate the NI-Index of Photovoltaic Panels

As required for the wind turbines, for the estimation of the visual impact index of the photovoltaic panels the tool requires the user to select the relative flag ("-f" using the CLI) also.

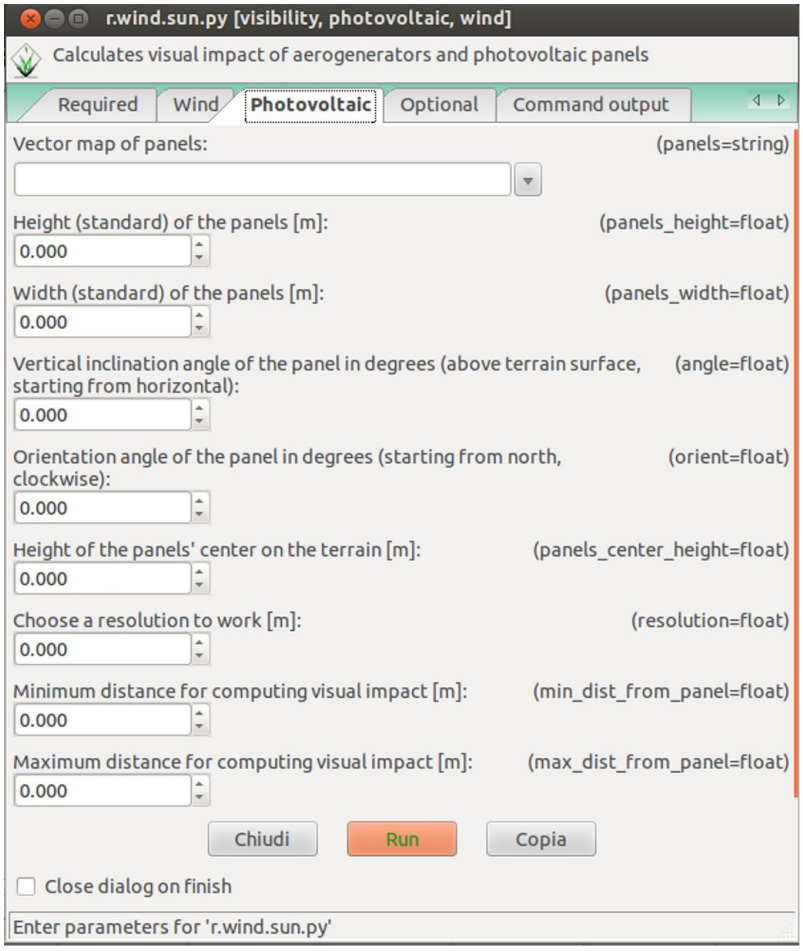

Figure II: The graphic user interface - "photovoltaic" tab.

The specific inputs for the photovoltaic analysis in the "photovoltaic" tab are:

- A point vector layer containing the position of the centroids of the panels.
- Height and width of the panel.
- Vertical inclination angle of the panel (expressed in degrees): calculated above the terrain, starting from the vertical position.
- orientation of the panel in degree: starting from north, clockwise.

- height of panel's center respect to the ground level.
- resolution of the final impact layer.
- maximum and minimum distance from the panel to evaluate visual impact.

Because most of the time, there are many elements (panels) in each photovoltaic field, it can be convenient to regroup contiguous panels as a "single element". In this case the dimensions and height of these grouped elements must be considered in place of those of a single panel.

The parameter "resolution of the final impact layer" allows the user to define a resolution to the output that may differ from the input resolution otherwise, it is inherited from the input DEM.

Here we show an example of the string required to execute the tool from the CLI:

r.wind.sun -f dem=dem impact=impactMap panels=placingPoints panels_height=panelHeight panels_width=panelWidth angle=panelInclin orient=panelOrient panels_center_height=panelHCT resolution=resolution min_dist_from_panel=4 max_dist_from_panel=10000

References

BISHOP, I. D., MILLER, D. R. *Visual assessment of off-shore wind turbines: The influence of distance, contrast, movement and social variables.* Renewable Energy, Volume 32, Issue 5, April 2007, Pages 814-831, ISSN 0960-1481, 10.1016/j.renene.2006.03.009.

CERRONI, S., VENZI, L.. *Confronto tra diverse localizzazioni di un impianto eolico contemperando produttività ed impatto visivo.* Pubblicazioni Ce.S.E.T., Italia, 0, (2009). URL: http://www.fupress.net/index.php/ceset/article/view/3225/2850. Access date 12 dec. 2012.

CHAMBERLAIN, B. C., MEITNER, M. J. *A route-based visibility analysis for landscape management.* Landscape and Urban Planning, Volume 111, March 2013, Pages 13-24, ISSN 0169-2046, 10.1016/j.landurbplan.2012.12.004.

CHIABRANDO, R., FABRIZIO, E., GARNERO, G. *On the applicability of the visual impact assessment OAISPP tool to photovoltaic plants.* Renewable and Sustainable Energy Reviews, Volume 15, Issue 1, January 2011, Pages 845-850, ISSN 1364-0321, 10.1016/j.rser.2010.09.030.

COSTELLA, J. P. *Galilean Antialiasing for Virtual Reality Displays.* sci.virtual-worlds (1992); University of Melbourne preprint UM–P–92/105.

CRAIK, K. H. *Multiple scientific paradigms in Environmental Psychology.* International Journal of Psychology, (1977) 12, 147- 157.

DE MONTIS, A., CASCHILLI, S. *Nuraghes and landscape planning: Coupling viewshed with complex network analysis.* Landscape and Urban Planning,

Volume 105, Issue 3, 15 April 2012, Pages 315-324, ISSN 0169-2046, 10.1016/j.landurbplan.2012.01.005.

DE RUBERTIS, R. *Fondamenti di geometria descrittiva.* Edizioni Kappa, (1979) Roma.

HURTADO J.P., FERNANDEZ J., PARRONDO J.L., BLANCO E. *Spanish method of visual impact evaluation in wind farms.* Renewable & Sustainable Energy Reviews (2003), 8,483–91.

IMRICH, J., PETLUS, P. Petluš 22 - *Development of a Program Tool for the Determination of the Landscape Visual Exposure Potential.* In: Ferenc Jordán and Sven Erik Jørgensen, Editor(s), Developments in Environmental Modelling, Elsevier, 2012, Volume 25, Pages 375-390, ISSN 0167-8892, ISBN 9780444593962, 10.1016/B978-0-444-59396-2.00022-5.

INCE, D. C., HATTON, L., GRAHAM-CUMMING, J. (2012). *The case for open computer programs.* Nature. doi:10.1038/nature10836.

KINDER, R. W., RALLINGS, P. J., WARE, J.A. *Parallel Processing for Terrain Analysis in GIS: Visibility as a Case Study.* Geoinformatica 1:2 (1997), pp. 183-207.

LADENBURG, J. *Visual impact assessment of offshore wind farms and prior experience.* Applied Energy, Volume 86, Issue 3, March 2009, Pages 380-387, ISSN 0306-2619, 10.1016/j.apenergy.2008.05.005.

LAKE, M.W., WOODMAN, P.E., MITHEN, S.J. *Tailoring GIS Software for Archaeological Applications: An Example Concerning Viewshed Analysis.* Journal of Archaeological Science, Volume 25, Issue 1, January 1998, Pages 27-38, ISSN 0305-4403, 10.1006/jasc.1997.0197.

Landscape Institute, Environmental Management Assessment *Guidelines for landscape and visual impact assessment (2nd ed.).* Spon Press (2002).

LEWIS, N. S, NOCERA, D. G., *Powering the Planet: Chemical Challenges in Solar Energy Utilisation*, 2006, Proceedings of the National Academy of Sciences of the United States of America, 103(43), 15729-15735, doi:10.1073/pnas.0603395103.

LONGELY, P. A., GOODCHILD, M., MAGUIRE, D. J., RHIND, D. W. *Geographic Information Systems and Science (3rd Edition)*, 2010, London: John Wiley & Sons

MANCHADO C., OTERO C., GOMEZ-JAUREGUI V., ARIAS R., BRUSCHI V., CENDRERO A. *Visibility analysis and visibility software for the optimisation of wind farm design.* Renewable Energy, Volume 60, December 2013, Pages 388-401, ISSN 0960-1481, http://dx.doi.org/10.1016/j.renene.2013.05.026.

MOELLER, B. *Changing wind-power landscapes: regional assessment of visual impact on land use and population in Northern Jutland, Denmark.* Applied Energy, Volume 83, Issue 5, May 2006, Pages 477-494, ISSN 0306-2619, 10.1016/j.apenergy.2005.04.004.

MOLINA-RUIZ, J., MARTINEZ-SANCHÉZ, M. J., PÉREZ-SIRVENT, C., TUDELA-SERRANO, M. L., & LORENZO, M. L. G. (2011) *Developing and applying a GIS-assisted approach to evaluate visual impact in wind farms.* Renewable Energy 36 (3), 1125-1132.

NETELER, M. *g.extension tool*. Geographical Resource Analysis Support Sysitem (GRASS) GIS. Open Source Geospatial Foundation Project (2012), http://grass.osgeo.org/grass64/manuals/g.extension.html.

NETELER, M., MITASOVA, H. *Open Source GIS: A GRASS GIS Approach.* Third Edition. The International Series in Engineering and Computer Science (2008). Volume 773. 406 pages, 80 illus., Springer, New York; ISBN: 038735767X.

PAINULY, J. P., *Barriers to Renewable Energy Penetration: a Framework for Analysis*, Renewable Energy, 2001, 24(1), 73 - 89

POL, E. *Blueprints for a History of Environmental Psychology (I): From First Birth to American Transition.* Medio Ambiente y Comportamiento Humano (2006), 7(2), 95-113. ISSN 1576-6462.

REGIONE AUTONOMA DELLA SARDEGNA *Linee guida per l'individuazione degli impatti potenziali degli impianti fotovoltaici e loro corretto inserimento nel territorio. Guidelines for the assessment of the potential impacts of photovoltaic systems and for the correct siting* (2008). Decree n. 30/2 on the 23 May 2008.

RODRIGUES, M., MONTANÉS, C., FUEYO, N. *A method for the assessment of the visual impact caused by the large-scale deployment of renewable-energy facilities.* Environmental Impact Assessment Review, Volume 30, Issue 4, July 2010, Pages 240-246, ISSN 0195-9255, 10.1016/j.eiar.2009.10.004.

ROGGE, E., NEVENS, F., GULINK, H. Reducing the visual impact of greenhouse parks in rural landscapes. Landscape and Urban Planning 87 (2008) 76–83.

Scottish Natural Heritage, Scottish Renewables Forum and The Scottish Society of Directors of Planning (2006). *Visual representation of windfarms. Good practice guidance.* http://www.snh.gov.uk/docs/A305436.pdf [accessed 05.09.2013]

SHANG, H., BISHOP, I.D., *Visual thresholds for detection, recognition and visual impact in landscape settings.* Journal of Environmental Psychology, Volume 20, Issue 2, June 2000, Pages 125-140, ISSN 0272-4944, 10.1006/jevp.1999.0153.

SPECTOR, R. H. *Visual Fields. Clinical Methods: The History, Physical, and Laboratory Examinations* (1990). 3rd edition. Boston: Butterworths; Chapter 116.

TOMA, L., ZHUANG, Y., RICHARD, W., METZ, M. *r.viewshed tool*. Geographical Resource Analysis Support Sysitem (GRASS) GIS. Open Source Geospatial Foundation Project (2012),

http://grass.osgeo.org/grass64/manuals/g.extension.html. Access date 13 dec. 2012.

TSOUTSOS, T., TSOUCHLARAKI, A., TSIROPOULOS, M., SERPETSIDAKIS, M. *Visual impact evaluation of a wind park in a Greek island.* Applied Energy, Volume 86, Issue 4, April 2009, Pages 546-553, ISSN 0306-2619, 10.1016/j.apenergy.2008.08.013.

TURNBULL, W. M., GOURLAY, I. *Visual impact analysis: a case study of a computer-based system.* Computer-Aided Design, Volume 19, Issue 4, May 1987, Pages 197-202, ISSN 0010-4485, 10.1016/0010-4485(87)90069-8.

VAN ROSSUM, G., DRAKE, F.L. *Python Reference Manual* (2001). PythonLabs, Virginia, USA . Available at http://www.python.org . Access date 12 dec. 2012.

VISSERING J., SINCLAIR M., MARGOLIS A. (2011). *A visual impact assessment process for wind energy projects.* State clean energy program guide (CESA) http://www.cleanenergystates.org/assets/2011-Files/States-Advancing-Wind-2/CESA-Visual-Impacts-Methodology-May2011.pdf [accessed 06.09.2013]

WÜSTENHAGEN, R., WOLSINK, M., BÜRER, M. J., *Social Acceptance of Renewable Energy Innovation: An Introduction to the Concept*, 2007, Energy Policy, 35(5), 2683 – 2691, http://dx.doi.org/10.1016/j.enpol.2006.12.001

		43